TaF_n and $TaCl_n$ Atomization Energies for $n = 1-5$

Charles W. Bauschlicher, Jr.

Mail Stop 230-3, NASA Ames Research Center, Moffett Field, California 94035

Received: December 9, 1999; In Final Form: April 14, 2000

TaF_n and $TaCl_n$ atomization energies are computed for $n = 1-5$. The geometries, frequencies, and atomization energies are determined using density functional theory. Both the BP86 and B3LYP functionals are used. Our best atomization energies are obtained by scaling the DFT results on the basis of the experimental TaX_5 atomization energies and including a correction for spin−orbit effects. For TaF_n, our corrected values are in good agreement with experiment. For TaF, TaCl, and $TaCl_2$ the atomization energies are also computed at the coupled cluster level of theory in conjunction with relativistic effective core potentials. The CCSD(T) complete basis set (CBS) limit is obtained by extrapolation. The scaled DFT values are in good agreement with these CCSD(T) CBS values. The TaF_n results and the calibration calculations suggest that the scaled $TaCl_n$ DFT atomization energies are accurate to 3−5 kcal/mol.

I. Introduction

$TaCl_5$ is used as a starting material in chemical vapor deposition (CVD) processes; for example, $TaCl_5(g) + {}^5/_2H_2(g) \rightarrow Ta(s) + 5HCl(g)$. To model such processes requires accurate heats of formation for $TaCl_5$ and all of its fragments. Unfortunately, the only reliable data is for the atomization energy of $TaCl_5$,[1] 512.10 ± 2.0 kcal/mol at 0 K. As discussed by Behrens and Feber,[2] the different determinations of the heat of formation of $TaCl_4$ differ by 12−25 kcal/mol. Using the $TaCl_5$ and $TaCl_4$ results, Behrens and Feber also estimated heats of formation for $TaCl_3$, $TaCl_2$, and TaCl.

While great progress has been made in computing accurate bond energies for molecules containing the atoms from the first three rows of the periodic table, the calculation of accurate bond energies for molecules containing atoms as heavy as Ta is a difficult problem, since both electron correlation and relativistic effects are expected to be important. All of the TaF_n bond energies, at 298 K, have been measured by Lau and Hildenbrand.[3] With an uncertainty of ±3 kcal/mol, the TaF_n values can be used to calibrate methods for treating systems containing Ta.

In this paper, we compute the bond energies of TaF_n and $TaCl_n$, $n = 1-5$, using density functional theory (DFT). We scale our DFT values using the experimental results for TaX_5 and include a correction for spin−orbit effects. The accuracy of this approach is tested using the experimental results for TaF_n. In addition, for TaF, TaCl, and $TaCl_2$, the DFT results are compared with the results of more accurate calculations.

II. Methods

The geometries are optimized using the BP86[4,5] and hybrid[6] B3LYP[7] functionals. The 6-31+G* basis set[8] is used for F and Cl and the Los Alamos effective core potential[9] (ECP) and associated double-ζ basis set (denoted LANL2DZ in Gaussian) are used for Ta. The harmonic frequencies confirm that the stationary points correspond to minima and are used to compute the zero-point energies. We should note that using the default "fine grid" results in small distortions away from the expected symmetry in some cases. This is avoided by using a larger grid with 96 radial points and 974 angular points.

A series of calibration calculations are performed for the diatomic and triatomic molecules in order to help establish the error in the DFT bond energies. One test involves all-electron self-consistent field (SCF) calculations on TaCl that include the scalar relativistic effects using the one-electron Douglas−Kroll (DK) approximation.[10] The Cl basis set is the augmented correlation consistent polarized valence triple-ζ (aug-cc-pVTZ) set[11−14] with the contraction coefficients taken from a DK atomic calculation. The Ta basis set is derived from the (29s24p15d9f) set optimized by Dyall.[15] The outermost three d functions are replaced by five even-tempered functions with a β of 2.1. A diffuse f function with an exponent of 0.207 714 and a g function with an exponent of 0.411 are added. This primitive set is contracted to [8s9p8d5f1g] on the basis of an atomic DK calculation on the $^4F(5d^36s^2)$ state of Ta.

For TaF, TaCl, and $TaCl_2$ the atomization energies are also computed using the restricted coupled cluster singles and doubles approach[16,17] including the effect of connected triples determined using perturbation theory,[18,19] RCCSD(T). In the RCCSD(T) calculations, the Ta 5d and 6s, the F 2s and 2p, and the chlorine 3s and 3p electrons are correlated. For F and Cl, the aug-cc-pV basis sets[11−14] are used. The triple-ζ (TZ), quadruple-ζ (QZ), and quintuple zeta (5Z) sets are used. For Ta we use the averaged relativistic effective core potential (ARECP) of Christiansen and co-workers,[20] which includes the 5s and 5p orbitals in the valence space, and the Stuttguart/Bonn 60MWB ECP.[21] The valence basis set is taken from the Dyall all-electron Ta set; the outermost 13 s primitives, 13 p primitives, and 10 d primitives (the most diffuse five being the even-tempered functions described above) are used. The innermost 10 s primitives, 9 p primitives, and 5 d primitives are contracted to two, one, and one functions, respectively, thus yielding a (13s13p10d)/[5s5p6d] set. Note that separate contraction coefficients are used for the two different ECPs. A series of cc-pV polarization sets are developed for correlating the five valence electrons for the Ta $^4F(5d^36s^2)$ state. The polarization sets are optimized at the singles and doubles configuration interaction (CI) level using the ARECP. The final polarization sets are given in Table 1. To improve the accuracy of the CCSD(T) results,

10.1021/jp994344r
Published on Web 05/31/2000

TABLE 1: Optimized Ta cc-pV Polarization Functions

type	terms	mean exponent	β
	TZ		
f	2	0.374	3.242
g	1	0.411	
	QZ		
f	3	0.376	2.604
g	2	0.482	3.119
h	1	0.506	
	5Z		
f	4	0.390	2.274
g	3	0.518	2.590
h	2	0.567	2.695
i	1	0.595	

we extrapolate to the complete basis set (CBS) limit using the two-point[22,23] and three-point[22] schemes.

The atomic spin−orbit contribution to the atomization energies is taken from experiment,[24] while the molecular spin−orbit effects are computed using the state-averaged complete-active-space SCF (SA-CASSCF)/valence CI approach. In the design of the CASSCF calculations, we assume that the systems are completely ionic (that is, Ta transfers one electron to each F or Cl) and only the nonbonding Ta electrons are correlated. Thus, for Ta, TaX, TaX_2, TaX_3, and TaX_4 there are 5, 4, 3, 2, and 1, active electrons, respectively. The active space in all SA-CASSCF calculations is the six Ta 5d and 6s orbitals. We should note that the systems are not completely ionic and therefore the active orbitals contain some F or Cl character.

The SA-CASSCF calculations include the lowest states, which are discussed for each molecule separately below. These SA-CASSCF orbitals are used in the valence CI calculations to compute the spin−orbit effects. The valence CI calculations use all configurations in the SA-CASSCF as references and add all single and double excitations out of the closed-shell valence orbitals into the active orbitals. Note that the Ta 5s and 5p electrons are not considered as valence electrons and therefore not correlated. The valence CI calculations include five roots of each symmetry, and the spin−orbit effect is computed from the interaction between all of the ΛS wave functions determined in the valence CI calculations. In some calculations the diagonal elements of the spin−orbit matrix are shifted based on higher level treatments; this is discussed on a case by case basis below. For TaX_3 and TaX_4, we included the highest inactive a_1 orbital from the CASSCF calculation in the valence CI active space in order to obtain a reasonable guess for all five states of each symmetry in the diagonalization procedure. For these systems, the Cl 3s or F 2s electrons are also excluded from the correlation treatment to make the calculations more tractable.

As we show below, the geometries obtained at all levels of theory are in reasonable agreement. Therefore, the calculation of the spin−orbit splitting is performed at the B3LYP geometry and applied to the both the B3LYP and BP86 results. We should note that for TaCl the spin−orbit splitting changed by less 40 cm^{-1} between the B3LYP and BP86 geometries. This is small compared with the uncertainty introduced by errors in the diagonal elements (even after applying our corrections) and uncertainty due to scaling the computed DFT results.

In these SA-CASSCF/valence CI calculations, the averaged and spin−orbit ECPs of Christiansen and co-workers[20,25] are used for Ta, F, and Cl. The F and Cl basis sets are derived from those of Christiansen and co-workers; a diffuse s (Cl 0.072 and F 0.103) and a diffuse p (Cl 0.073 and F 0.119) function are added to the (4s4p) set. These expanded sets are contracted to [4s4p] for Cl and [3s3p] for F. The 3d2f polarization functions from the aug-cc-pVTZ sets are added. The Ta valence basis set is derived from the (22s16p13d8f) all-electron basis set optimized by Faegri.[26] The outermost seven s, six p, and five d functions are used for the ECP valence basis set and supplemented with three p (0.121, 0.055, and 0.025) and two d (0.058 and 0.026) functions. This valence set is contracted to [4s5p5d]; the inner five s primitives are contracted to two functions, the inner five p primitives to one, and the inner three d primitives to one function, with the remaining primitives uncontracted. A 2f1g polarization set is added; the f functions are even tempered with $\beta = 3.252$ and a mean exponent of 0.37, while the g function has an exponent of 0.42.

TABLE 2: Optimized Geometries: Bond Lengths (in Å) and Angles (in deg)

	BP86	B3LYP	BP86	B3LYP
	TaF		TaCl	
$r(^5\Pi)$	1.936	1.942	2.305	2.325
$r(^3\Phi)$	1.876	1.882	2.276	2.287
$r(^3\Sigma^-)$	1.811	1.815	2.238	2.251
	TaF_2		$TaCl_2$	
$r(^4\Sigma_g^-)$	1.882	1.882	2.298	2.307
$r(^2\Delta_g)$	1.879[a]	1.878	2.265	2.272
	TaF_3		$TaCl_3$	
$r(^1A'_1)$ $^3A_2$[b]	1.841	1.840	2.249	2.255
$r(=)$	1.889	1.887	2.299	2.307
r	1.866	1.864	2.281	2.275
ang(=)	129.1	129.0	126.6	126.3
	TaF_4		$TaCl_4$	
r ($^2A_1$)	1.870	1.866	2.292	2.294
angle[c]	141.2	141.1	126.0	123.8
	TaF_5		$TaCl_5$	
$r(^1A'_1)$(axial)[d]	1.889	1.879	2.345	2.343
r(equatorial)	1.855	1.847	2.297	2.296

[a] Bent with FTaF angle of 168.7°. [b] The molecule has C_{2v} with two equivalent Ta-X bond, labeled $r(=)$ and two equivalent angles, ang(=). [c] The molecule has D_{2d} symmetry. All of the bond lengths are equivalent. There are six XTaX angles, four with one value and two with the second value; we report the latter angle. [d] The molecule has D_{3h} symmetry.

The DFT calculations are performed using Gaussian 94[27] or Gaussian 98.[28] The spin−orbit CASSCF/valence CI calculations and CCSD(T) calculations are performed using Molpro.[29] The DK SCF calculations are performed using Molecule-Sweden.[30] The DK integrals are computed using a modified version of the program written by Hess.

The heat capacity, entropy, and temperature dependence of the heat of formation are computed for 300−4000 K using a rigid rotor/harmonic oscillator approximation. The DFT frequencies are used in these calculations. The effect of low-lying electronic states is accounted for using the valence CI spin−orbit levels, except for Ta, F, and Cl, where experiment is used. These results are fit in two temperature ranges, 300−1000 and 1000−4000 K, using the Chemkin[31] fitting program and following their constrained three step procedure.

III. Results and Discussion

A. Determination of the Ground State. The geometries are optimized at the B3LYP and BP86 levels of theory, and the results are summarized in Table 2. The computed DFT harmonic frequencies are given in Table 3. In general, several states are studied for each molecule and in some cases multiple structures are considered. In addition to those structures reported in the tables, a few of the more noteworthy structures tried at the B3LYP level of theory include nonlinear $TaCl_2$ for both the doublet and quartet states, square planar and tetrahedral structures for the doublet state of $TaCl_4$, and a square pyramidal

TABLE 3: Computed Harmonic Frequencies (in cm^{-1}) and Intensities (in km/mol, in Parentheses)

	BP86	B3LYP	BP86	B3LYP
	TaF		TaCl	
$^5\Pi$	599(148)	596(157)	357(32)	348(37)
$^3\Phi$	654(105)	651(117)	375(27)	372(32)
$^3\Sigma^-$	737(35)	738(50)	384(7)	380(14)
	TaF_2		$TaCl_2$	
$^4\Sigma_g^-$				
π	34(7)	49(10)	36(3)	37(5)
σ_u	653(240)	660(258)	381(130)	376(143)
σ_g	677(0)	683(0)	361(0)	359(0)
$^2\Delta_g$				
π	41(3)	36(9)	35(0.6)	41(2)
σ_u	659(233)	664(257)	395(112)	391(127)
σ_g	681(2)	686(0)	380(0)	378(0)
	TaF_3		$TaCl_3$	
$^1A'_1$				
e′	156(5)	158(8)	84(0)	88(0.2)
a''_2	160(0)	166(1)	96(0.2)	97(0)
a'_1	717(0)	727(0)	384(0)	384(0)
e′	723(255)	734(296)	407(120)	407(145)
$^3A_2$				
b_2	52(15)	46(20)	33(8)	31(11)
b_1	124(5)	130(8)	71(2)	73(3)
a_1	178(3)	180(5)	100(0)	99(0.2)
b_2	593(148)	601(163)	344(114)	339(127)
a_1	674(53)	686(57)	365(0.4)	365(0.6)
a_1	690(137)	701(154)	397(83)	396(94)
	TaF_4		$TaCl_4$	
a_1	159(0)	158(0)	71(0)	70(0)
b_2	162(7)	167(12)	87(2)	87(4)
e	163(31)	169(40)	106(5)	107(7)
b_1	237(0)	241(0)	131(0)	128(0)
b_2	660(49)	672(57)	366(47)	367(60)
a_1	699(0)	717(0)	373(0)	376(0)
e	678(408)	694(257)	382(180)	385(195)
	TaF_5		$TaCl_5$	
e′	102(6)	105(6)	59(3)	59(4)
e′	198(44)	206(55)	138(9)	140(11)
a''_2	249(23)	259(28)	169(10)	171(12)
e″	277(0)	284(0)	188(0)	191(0)
a'_1	630(0)	649(0)	305(0)	305(0)
a''_2	656(277)	675(309)	352(143)	353(167)
e′	711(338)	732(381)	380(145)	382(179)
a'_1	724(0)	749(0)	378(0)	385(0)

structure for the singlet state of $TaCl_5$. These structures were not minima, and either collapsed to the structures reported or had an imaginary frequency. For those systems with an imaginary frequency, when the geometry was displaced in the direction of the imaginary mode, the geometry collapsed to the structures reported.

In some cases, the separations between the states were also computed at the CCSD(T) level of theory. CASSCF/valence CI calculations were used to compute the spin−orbit effects, and these calculations were performed at the B3LYP optimized geometries. On the basis of the DFT, CCSD(T), and CASSCF/valence CI calculations, the ground state was determined. In this subsection we discuss using this procedure to determine the ground state, while in the next subsection we consider the determination of the best atomization energies.

The ground state of Ta is $^4F(5d^36s^2)$, while the $^6D(5d^46s^1)$ excited state is significantly higher in energy, namely 23.9 kcal/mol higher using the weighted average of the J states. The B3LYP approach yields 22.04 kcal/mol, which is in good agreement with experiment, while BP86 places the ^6D too close to the ^4F state, yielding a separation of 12.74 kcal/mol. At the valence CI level, the spin−orbit lowering, i.e., the difference between the LS and lowest J levels, is 3527 cm^{-1}, which is in good agreement with the experimental value[24] of 3571 cm^{-1}, especially in light of the simplicity of the approach. We should note that the analogous values for F and Cl are 62 and 163 cm^{-1}, respectively, which do not compare that favorably with the experimental values of 135 and 294 cm^{-1}. However, the open-shell character in TaX_n should be localized mostly on Ta, so we believe that the error in the F or Cl spin−orbit lowering should not significantly affect the molecular spin−orbit results. Remember that the larger atomic spin−orbit effects are computed using experiment.

TABLE 4: CCSD(T) Results for TaX Using the ARECP of Christensen and Co-workers

state	r_e (Å)	D_e (kcal/mol)	ω_e (cm^{-1})	T_e (cm^{-1})
		TaCl TZ		
$^3\Sigma^-$	2.251	99.02	401	0
$^3\Phi$	2.281	97.32	388	594
$^5\Pi$	2.313	92.69	364	2213
$^5\Delta$	2.315	90.84	363	2860
		TaCl QZ		
$^3\Sigma^-$	2.246	101.58	403	0
$^3\Phi$	2.275	99.98	388	563
		TaCl 5Z		
$^3\Phi$	2.271	101.21	388	
		TaF TZ		
$^3\Sigma^-$	1.840	141.18	697	0
$^3\Phi$	1.884	132.93	666	2885
$^5\Pi$	1.907	125.27	626	5567
$^5\Delta$	1.955	115.71	592	8909
		TaF QZ		
$^3\Sigma^-$	1.839	143.01	703	0
$^3\Phi$	1.882	134.78	671	2879
$^5\Pi$	1.906	127.00	630	5597
		TaF 5Z		
$^3\Sigma^-$	1.840	143.62	704	0
$^3\Phi$	1.882	135.45	675	2857
$^5\Pi$	1.906	127.52	631	5631

If the bonding in TaCl arises from the ^4F state of Ta, we expect sp and/or sd hybridization of the Ta and the formation of a Ta−Cl bond between the Ta hybrid and the Cl open-shell 3p orbitals. The other hybrid orbital can be high- or low-spin coupled to the open-shell 5d orbitals, giving rise to either triplet or quintet states. In the triplet states, the dσ is occupied to allow for sd hybridization and some d character in the Ta−Cl bond. Therefore, the open-shell 5d occupation can be either $5d\pi^15d\delta^1$ or $5d\pi^2$, giving rise to a $^3\Phi$ or $^3\Sigma^-$ state, respectively. The $^3\Phi$ state has the benefit of being derived from Ta ^4F, while the $^3\Sigma^-$ reduces the repulsion between the Ta π and Cl π orbitals and allows more Cl π donation into the empty Ta d orbitals. The lowest state of TaCl arising from the Ta ^6D state is expected to be a quintet, where the 6s orbital forms a bond with Cl 3p orbital. Since a quintet state also arises from Ta ^4F when the hybrid orbital is high-spin coupled to the open-shell d orbitals, it is not surprising that the lowest TaCl quintet state is a mixture of the states arising from Ta ^4F and ^6D.

The $^3\Sigma^-$, $^3\Phi$, $^5\Delta$, and $^5\Pi$ states of TaCl are considered at the CCSD(T) level using the ARECP and the cc-pV basis sets, and the results are summarized in Table 4. The lowest state is $^3\Sigma^-$, but the $^3\Phi$ state is low-lying. The quintet states are higher in energy. At the B3LYP level the $^3\Phi$ state is below the $^3\Sigma^-$ state, and the $^3\Phi$ state is below the $^5\Pi$ state. At the BP86 level, the $^3\Phi$ and $^5\Pi$ states are virtually degenerate, which is probably a result of the BP86 approach having the ^6D state of Ta too low relative to the ^4F state. The difference between the DFT and CCSD(T) results are summarized in Figure 1.

Spin−orbit effects for TaCl were computed at the $^3\Phi$ and $^5\Pi$ geometries for several choices of the states included in the

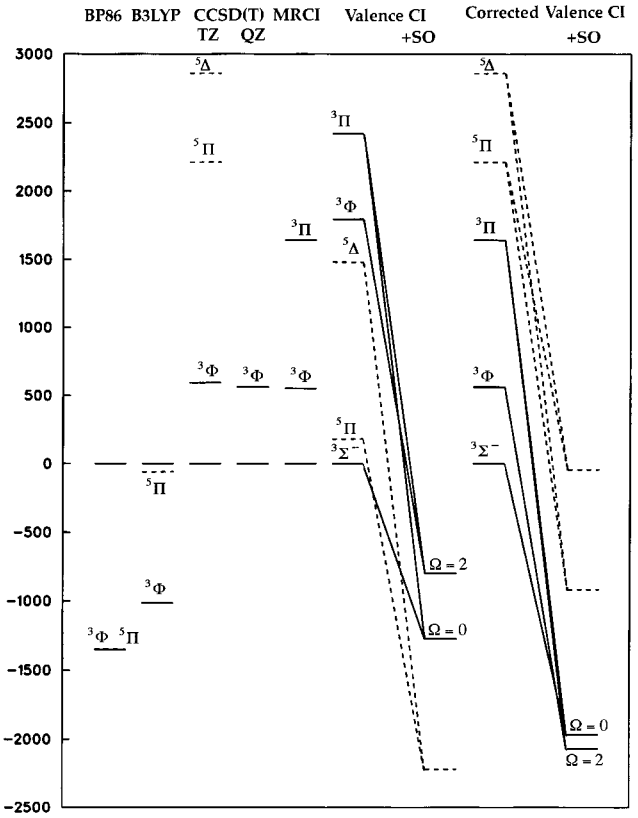

Figure 1. Relative separation between selected low-lying states of TaCl as a function of level of theory. The quintet states are dashed lines while the triplet states are solid lines. Note that for the BP86 approach the $^3\Phi$ and $^5\Pi$ states are essentially degenerate, and therefore appear as one line. In the results presented for the valence CI + spin−orbit approach, the spin−orbit lower was computed separately for the triplet and quintet states. In the results presented for the corrected valence CI + spin−orbit approach, the triplet and quintet states were treated simultaneously in the spin−orbit treatment. The first three roots (two of which are shown) are mostly triplet in character, while the fourth and fifth (shown as dashed lines) roots are mostly quintet in character.

SA-CASSCF procedure. While the final spin−orbit calculation included both the triplet and quintet states, the initial calculations included only the triplet states or only the quintet states, in order to obtain insight into the spin−orbit effects. At the $^5\Pi$ geometry and including the $^5\Sigma^+$, $^5\Pi$, and $^5\Delta$ states in the SA-CASSCF procedure, the valence CI places the $^5\Pi_0$ state 2149 cm^{-1} below the $^5\Pi$ ΛS state. This $\Omega = 0$ state is a mixture of the $^5\Pi$, $^5\Delta$, and $^5\Sigma^-$ ΛS states. In the absence of the mixing of the quintet states, the $^5\Pi_{-1}$ component would have been expected to be the lowest in energy; a state with this character is found to be 416 cm^{-1} above the $\Omega = 0$ state. Since the spin−orbit lowering of the $^5\Pi$ state is smaller than the separation between $^3\Sigma^-$ and $^5\Pi$ states, the ground state must be derived from the triplet states, and therefore we focus on the spin−orbit splitting in the triplet states.

At the B3LYP $^3\Phi$ geometry, the orbitals are optimized including the $^3\Phi$, $^3\Pi$, and $^3\Sigma^-$ states in the SA-CASSCF calculation. This is followed by the valence CI calculations. Including only the triplet states in the spin−orbit calculation results in a $\Omega = 0$ ground state that is derived from a mixing of the $^3\Sigma^-$ and $^3\Pi$ states. This $\Omega = 0$ state is 1272 cm^{-1} below the $^3\Sigma^-$ ΛS state. The $\Omega = 2$ state, which is derived mostly from the $^3\Phi$ state, is 474 cm^{-1} above the $\Omega = 0$ state. However, the valence CI places the $^3\Sigma^-$ state 1794 cm^{-1} below the $^3\Phi$ state, compared with the best CCSD(T) calculation, which places the $^3\Sigma^-$ state only 563 cm^{-1} below the $^3\Phi$. The limitations of the valence CI can be seen in Figure 1. Since the $\Omega = 2$ state is mostly derived from $^3\Phi$ and the $\Omega = 0$ state is mostly derived from $^3\Sigma^-$, the CCSD(T) separations suggest that the $\Omega = 2$ and $\Omega = 0$ states would reverse if the separation between the $^3\Sigma^-$ and $^3\Phi$ states is improved from the valence CI value to the CCSD(T) value. However, it should be noted that the $^3\Pi$ state, which mixes with the $^3\Sigma^-$ state to produce the $\Omega = 0$ state, is not positioned correctly at the valence CI level either. While we do not have a CCSD(T) value for this state, a multireference (MR) CI treatment yields a $^3\Sigma^- - ^3\Pi$ separation of 1642 cm^{-1} compared with a valence CI value of 2421 cm^{-1}. Note that the $^3\Sigma^- - ^3\Phi$ separation from this MRCI calculation is 551 cm^{-1}, which is in excellent agreement with the CCSD(T) value. A further complication in the calculation of the spin−orbit splitting at the valence CI level is the fact that the lowest quintet state is below the $^3\Phi$ state and only 180 cm^{-1} above the $^3\Sigma^-$, leading to the lowest state of the quintet spin−orbit treatment being far below the lowest state of the triplet spin−orbit treatment.

To correct for these problems, the spin−orbit calculations are repeated, but with the diagonal elements shifted to account for the known limitation of the valence CI. That is, the $^3\Phi$ state is shifted down to reproduce the CCSD(T)/QZ $^3\Sigma^- - ^3\Phi$ separation (563 cm^{-1}) and the $^3\Pi$ state is shifted to reproduce the MRCI $^3\Sigma^- - ^3\Phi$ separation. After these shifts, the $\Omega = 2$ state is 2580 cm^{-1} below the $^3\Phi$ and the $\Omega = 0$ state is 1582 cm^{-1} below the $^3\Sigma^-$, and thus the $\Omega = 2$ state is 435 cm^{-1} below the $\Omega = 0$ state. We next add the quintet states to the spin−orbit calculation. In these calculations, $^5\Sigma^+$ and $^5\Delta$ states and the $^5\Pi$ and $^5\Phi$ states are shifted by the difference between the valence CI and CCSD(T)/TZ results for the $^3\Sigma^- - (1)^5\Delta$ and $^3\Sigma^- - (1)^5\Pi$ separations, respectively. When the quintet states are included, the $^3\Phi$ state splitting is increased to 2636 cm^{-1} and the $\Omega = 0$ state is now only 110 cm^{-1} above the $\Omega = 2$ state. While it is clear that the ground state is derived from the triplets, this separation is too small for us to definitively determine if the ground state is $\Omega = 0$ or $\Omega = 2$. We computed the atomization energy by adding 2636 cm^{-1} to our best DFT $^3\Phi$ result.

Analogous calculations are performed for TaF, where the $^3\Sigma^-$ state is found to be much more stable relative to the other states than found for TaCl—see Table 4. The final spin−orbit lowering is computed after correcting the diagonal elements of the SA-CASSCF/valence CI spin−orbit matrix as was done for TaCl. Because of the much larger separation between the ΛS states, spin−orbit effects lower the $^3\Sigma^-$ state by only 826 cm^{-1}; this is much smaller than found for TaCl. We compute the TaF binding energy by adding 826 cm^{-1} to our DFT results for the $^3\Sigma^-$ state.

The ground state of $TaCl_2$ is $^4\Sigma_g^-$ at all levels of theory. The bonding in this state can be viewed as arising from $^4F(5d\sigma^1 5d\delta^2 6s^2)$, where 6s6p hybridization occurs and two Ta−Cl bonds are formed. An inspection of the orbitals shows that the bonds are polarized toward the Cl (i.e., there is a large ionic component to the bonding) and there is also mixing of the 5dσ and 6s orbitals. Since $d\sigma^1 d\pi^1 d\delta^1$ is 100% ^4F, while $d\sigma^1 d\delta^2$ is 80% ^4F and 20% ^4P, the $^4\Phi_g$ state might have been expected to be below the $^4\Sigma_g^-$, but minimizing the repulsion between the Cl 3pπ orbitals and the Ta 5dπ orbitals must be more important than the more favorable Ta atomic coupling.

The lowest doublet state is found to be $^2\Delta_g$, which as shown in Table 5, is very low-lying; clearly spin−orbit effects must be accounted for in the determination of the ground state. At the valence CI level, mixing only the quartet states, the $^4\Sigma_g^-$ state is lowered by 532 cm^{-1} due to mixing with the $^4\Pi_g$ state. When only the doublet states are considered, the lowest Ω

TABLE 5: CCSD(T) Results for TaX_2 Using the ARECP of Christensen and Co-workers

state	r_e (Å)	T_e (cm^{-1})
	$TaCl_2$ TZ	
$^4\Sigma_g^-$	2.303	0
$^2\Delta_g$	2.270	1000
	$TaCl_2$ QZ	
$^4\Sigma_g^-$	2.300	0
$^2\Delta_g$	2.268	948
	$TaCl_2$ 5Z	
$^4\Sigma_g^-$	2.297	0
$^2\Delta_g$	2.265	874
	TaF_2 TZ	
$^4\Sigma_g^-$	1.897	0
$^2\Delta_g$	1.874	520

component is 1975 cm^{-1} below the $^2\Delta_g$ ΛS state. In order to consider the simultaneous interaction of the quartet and doublet states, we shift all of the doublet diagonal elements by the difference between the valence CI and CCSD(T)/5Z $^4\Sigma_g^- - ^2\Delta_g$ separations. At this level, the $^4\Sigma_g^-$ derived state is lowered by 1394 cm^{-1} and the $^2\Delta_g$ derived state by 2341 cm^{-1}, which places the $^2\Delta_g$ derived state 73 cm^{-1} below the $^4\Sigma_g^-$ derived state. Clearly, we cannot unambiguously determine the ground state; therefore, to compute the energetics, we study the $^4\Sigma_g^-$ state at the DFT level and add 1400 cm^{-1} to account for spin−orbit splitting.

As shown in Table 5, for TaF_2 the $^2\Delta_g$ state is only 520 cm^{-1} above the $^4\Sigma_g^-$ state. These two states are essentially degenerate after spin−orbit effects are included (with the diagonal elements shifted using the CCSD(T) results as was done for $TaCl_2$) and thus the calculations are not sufficiently accurate to determine which is the ground state. To determine the energetics of TaF_2, we add our computed spin−orbit lowering of 1365 cm^{-1} to our $^4\Sigma_g^-$ DFT results. That is, the spin−orbit effects in TaF_2 and $TaCl_2$ are very similar, in contrast to the large difference found for TaF and TaCl.

$TaCl_3$ is a very interesting case. There are two low-lying states, one singlet and one triplet. The $^1A'_1$ state has D_{3h} symmetry, with the doubly occupied nonbonding orbital being an sd hybrid above and below the plane of the molecule. The triplet state is formed by exciting one of the nonbonding electrons into the e″(dπ) orbital, thus yielding a $^3E''$ state. This state naturally undergoes a Jahn−Teller distortion yielding a planar $^3A_2$ state with C_{2v} symmetry. We note that the $^3A'_2$ state formed by doubly occupying the e″(dπ) orbital is higher in energy. Since the $^1A'_1$ and $^3E''$ states differ by a single spin−orbital, there is a large spin−orbit matrix element. Thus, to determine the ground state, we must consider both the spin−orbit and Jahn−Teller effects.

At the DFT level, the $^3A_2$ state is slightly below the $^1A_1'$ state, while at the CCSD(T) level of theory the ground state is $^1A'_1$ by 83 cm^{-1}. We should note that at the singlet geometry, the $^3B_1$ and $^3A_2$ components of the $^3E''$ are virtually degenerate at the SCF level, as expected, but the $^3B_1$ component is 632 cm^{-1} below the $^3A_2$ component at the CCSD(T) level, even though these two states should be degenerate for this D_{3h} geometry. Thus, the 83 cm^{-1} energy separation between the $^3A_2$ and $^1A'_1$ states is small compared with the nonphysical splitting in the two components of the $^3E''$ state at a D_{3h} geometry, and therefore it is not possible to definitively predict the separation between the $^3A_2$ and $^1A'_1$ states.

At the $^1A'_1$ state geometry (i.e., D_{3h}), $^3E''$ is below the $^1A'_1$ state at the SA-CASSCF and valence CI levels. This is to be compared with the CCSD(T) approach, where the $^1A'_1$ state is 1785 and 1153 cm^{-1} below the two components of the $^3E''$ state. Unlike the CCSD(T), the two components of the $^3E''$ state are degenerate at the SA-CASSCF level and differ by only 31 cm^{-1} at the valence CI level. As with TaCl and $TaCl_2$, we must shift the manifold of singlet and triplet states to obtain our best value for the spin−orbit splitting. At the $^1A'_1$ D_{3h} geometry, we shift all of the triplet states by the difference between the valence CI and CCSD(T) approaches for separation between the $^1A'_1$ and the $^3B_1$ component of the $^3E''$. The lowest spin−orbit component is 2583 cm^{-1} below the $^1A'_1$ state and is very mixed in character, containing 44% singlet and 56% triplet. At the $^3A_2$ C_{2v} geometry, we shift the triplet manifold by the error in the valence CI for the $^1A_1-^3A_2$ separation, and the lowest spin−orbit component is computed to be 2759 cm^{-1} below the $^1A_1$ state. Lowering the symmetry splits the $^3E''$ state into two components, one of which shifts down closer to the $^1A_1$ state and the other shifts away from the $^1A_1$ state. As a result, the spin−orbit splitting at the C_{2v} geometry is only slightly larger that at the D_{3h} geometry. This small increase in the spin−orbit effect is much smaller than the energy required (1008 cm^{-1} at the CCSD(T) level) to deform the $^1A'_1$ state to the C_{2v} structure. Therefore, $TaCl_3$ should have D_{3h} symmetry even though the ground state is more triplet than singlet. To compute the energetics we use the $^1A'_1$ DFT results, which we correct by 2583 cm^{-1} to account for spin−orbit effects.

TaF_3 has the same low-lying states as $TaCl_3$, but the separation between the $^1A'_1$ and $^3E''$ states is 7622 cm^{-1} at the CCSD(T) level using the TZ basis set. At both the B3LYP and BP86 levels, the $^1A'_1$ is also significantly below the distorted triplet state. Given the enhanced stability of the $^1A'_1$ state relative to the triplet state in TaF_3, is it not surprising that the computed spin−orbit lowering of the $^1A'_1$ state is only 773 cm^{-1}.

The optimal $TaCl_4$ structure has D_{2d} symmetry and is best viewed as arising from a distortion of the ^2E state of the T_d structure. The SA-CASSCF calculations, which are performed in C_{2v} symmetry, include three $^2A_1$, one $^2B_1$, one $^2B_2$, and one $^2A_2$ state in the averaging procedure. The spin−orbit splitting at the valence CI level is 584 cm^{-1}. This is much smaller than the separation (4086 cm^{-1}) between the two lowest states in the spin−orbit calculation, and therefore we conclude that the ground state is derived from the $^2A_1$ state. We compute the energetics using the DFT results for the $^2A_1$ state and add on 584 cm^{-1} to account for spin−orbit effects. The analogous TaF_4 calculations lead to a spin−orbit lowering of 304 cm^{-1}.

$TaCl_5$ and TaF_5 are closed-shell trigonal bipyramids, as expected. There are no first-order spin−orbit effects since they are closed shells. We ignore any molecular second-order effects. As shown in Tables 2 and 3, the B3LYP and BP86 frequencies and geometries are in excellent agreement. The frequencies agree with the summary in Behrens and Feber[2] to within about 20 cm^{-1} in the worst case. Our axial Ta−Cl bond length of 2.34 or 2.35 Å is slightly shorter than the experimental value[2] of 2.37 Å, while our equatorial value 2.30 Å is longer than the experimental value of 2.23 Å.

B. Atomization Energies. The TaF_n atomization energies (AEs) and bond energies (BEs) are summarized in Tables 6 and 7 along with the experimental results of Lau and Hildenbrand.[3] The computed values are corrected to 298 K using the computed geometries, frequencies, and spin−orbit energy levels. The unscaled B3LYP values (column 2 in Tables 6 and 7) are too small and adding on the spin−orbit effects (column 3) makes the agreement with experiment even worse. The BP86 values are too large and therefore adding the spin−orbit effects

TABLE 6: Computed TaF_n Atomization Energies at 298 K (in kcal/mol)

	unscaled		scaled[a]		
n	no SO[b]	+SO	no SO	+SO	expt[3]
			B3LYP		
1	134.4	126.1	137.3	131.4	137.0[c]
2	289.4	282.3	295.8	293.8	294.0
3	431.8	422.7	441.4	439.8	438.0
4	560.9	550.0	573.3	572.3	568.0
5	690.7	678.6	706.0	706.0	706.0
			BP86		
1	144.1	135.9	139.6	133.7	137.0
2	306.9	299.8	297.2	295.2	294.0
3	454.8	445.7	440.5	438.9	438.0
4	591.3	580.4	572.7	571.6	568.0
5	729.0	716.8	706.0	706.0	706.0

[a] The results are scaled so that the $n = 5$ values equal experiment. [b] Indicates that spin−orbit effects are not explicitly accounted for. [c] The CCSD(T)/CBS 298 K value including spin−orbit effects is 135.7 kcal/mol.

TABLE 7: Computed TaF_n Bond Energies at 298 K (in kcal/mol)

	unscaled		scaled[a]		
n	no SO	+SO	no SO	+SO	expt[3]
			B3LYP		
1	134.3	126.1	137.3	131.4	137.0
2	155.1	156.2	158.5	162.4	157.0
3	142.4	140.3	145.6	146.0	144.0
4	129.1	127.4	131.9	132.5	130.0
5	129.8	128.6	132.7	133.7	138.0
			BP86		
1	144.1	135.9	139.6	133.7	137.0
2	162.8	163.9	157.6	161.5	157.0
3	147.9	145.9	143.3	143.7	144.0
4	136.5	134.7	132.2	132.7	130.0
5	137.7	136.4	133.4	134.4	138.0

[a] The results are scaled so that the $TaCl_5$ atomization energy equals experiment.

improves the agreement with experiment, but the errors are still sizable. The individual bond energies all tend to be slightly large, which results in a sizable error in the atomization energies of TaF_3, TaF_4, and TaF_5. Scaling the computed results (column 4) by the ratio of the experimental to computed TaF_5 atomization energy improves the results significantly, with the maximum error being about 5 kcal/mol for both the BP86 and B3LYP approaches. This is reasonably good, especially if one considers the uncertainty in the experimental values is about ±3 kcal/mol.

Scaling the computed results attempts to account for all of the limitations in the calculations, but assumes that all of the errors increase with increasing atomization energy. However, some errors, such as spin−orbit effects, do not scale with the atomization energy. The atomic spin−orbit contribution is dominated by Ta, and therefore this contribution grows slowly with the number of F atoms. The molecular spin−orbit effect in general decreases with number of F atoms. Thus, the spin−orbit effects do not, in general, follow the atomization energies. We attempt to overcome this limitation of the scaling procedure by removing the spin−orbit effect from the experimental TaF_5 atomization energy, and scale the computed results by the ratio of this modified TaF_5 experimental value to the computed TaF_5 value. We then add back the spin−orbit effects to these new scaled results. These results are given the fifth column in Tables 6 and 7. For the B3LYP approach, the scaled results, with and without the spin−orbit effects, have about the same average absolute error. While the error in the scaled BP86 results is larger than in the scaled B3LYP results, once the spin−orbit effect is explicitly included, the scaled BP86+SO results have the smallest absolute error of the four scaling approaches. On the basis of the agreement with experiment, we conclude that the scaled BP86+SO approach yields an error of 3−5 kcal/mol in the computed atomization energies.

TABLE 8: Computed $TaCl_n$ Atomization Energies (in kcal/mol)

	without explicit spin−orbit				with SO		
	unscaled		scaled[a]		scaled		
	B3LYP	BP86	B3LYP	BP86	B3LYP	BP86	CCSD(T)/CBS
TaCl	87.9	97.9	97.4	99.3	96.8	98.7	98.1[b]
$TaCl_2$	205.3	221.6	224.2	224.6	222.1	222.4	223.4
$TaCl_3$	301.3	323.0	327.2	324.5	330.5	327.8	
$TaCl_4$	393.8	422.7	431.7	428.6	429.7	426.6	
$TaCl_5$	464.8	504.7	512.1	512.1	512.1	512.1	

[a] The values are scaled using the ratio of the experimental atomization energy and the DFT result for $TaCl_5$; see the text. [b] The CCSD(T)/CBS value using the Stuttgart/Bonn ECP is 96.3 kcal/mol.

Using the cc-pV{TZ,QZ,5Z} basis sets, the CCSD(T)/CBS dissociation energy of the $^3\Sigma^-$ state of TaF is computed. The three-point and two-point {QZ,5Z} methods yield very similar results, and we take the $n^{-4} + n^{-6}$ value[22] as our best result. This is corrected for zero-point energy using the CCSD(T) harmonic frequency, atomic spin−orbit effects using experiment,[24] molecular spin−orbit effects (using our SA-CASSCF/valence CI value described above), and for temperature. The final value of 135.7 kcal/mol is in good agreement with experiment and our scaled BP86+SO value. This is taken as additional support for the accuracy of the scaled BP86+SO result.

While the comparison of the TaF_n results with experiment supports our scaling approach, we perform additional calibration calculations for $TaCl_n$, because there is only one accurate experimental value; that is, we can compute a scale factor, but experiment does not give any confirmation of this approach for the $TaCl_n$ species.

Our first calibration calculation is designed to test our choice for the ECP. The all-electron atomization energy at the SCF level using the Douglas−Kroll approximation is 67.65 kcal/mol, compared with 68.01 kcal/mol using the TZ basis set and the Christiansen ECP and 64.75 kcal/mol using the Stuttgart ECP. The difference in the computed dissociation for the two ECPs is similar at the CCSD(T) and SCF levels of theory. Thus, we use the Christiansen ARECP for the higher level benchmark calculations.

The atomization energy of $TaCl_5$ is known[1] to be 512.10 ± 2.0 kcal/mol. As found for TaF_5, neither the BP86 result nor the B3LYP result has the desired accuracy. We follow the approaches used for TaF_n and scale the computed DFT values based on the ratio $TaCl_5$(expt)/$TaCl_5$(DFT). We also use the approach where spin−orbit effects are accounted for explicitly. That is, we scale the computed results by the ratio ($TaCl_5$ spin−orbit)/$TaCl_5$(DFT) and then add on the computed spin−orbit effects. These results are summarized in Table 8.

All of the scaled DFT values for TaCl and $TaCl_2$ agree with the CCSD(T) CBS values to within 2 kcal/mol. As with TaF_n, there is not an enormous variation in atomization between the four scaling approaches. On the basis of the TaF_n results, we pick the scaled BP86+SO as our best result. These scaled BP86+SO atomization energies are converted to 298 K and used to compute heats of formation—see Table 9. Our computed heat of formation for $TaCl_4$ differs by about 12 kcal/mol from

TABLE 9: Heats of Formation[a] and Bond Energies (in kcal/mol)

	AE(0)	AE(298)	BE(298)	ΔH^b	ΔH(expt[c])	BE(expt)
TaCl	98.7	99.3	99.3	116.6	86.0	129.8
$TaCl_2$	222.4	223.2	123.9	21.6	−16.0	131.0
$TaCl_3$	327.8	329.4	106.2	−55.6	−77.0	90.0
$TaCl_4$	426.6	428.6	99.3	−125.7	−137.1	89.1
$TaCl_5$	512.1	514.7	86.1	−182.8	−182.8	74.4

[a] Determined using the Ta and Cl heats of formation, 28.99 and 186.90 kcal/mol, respectively. [b] The computed atomization energies have been scaled so that $TaCl_5$ atomization energy agrees with experiment. [c] The values for TaCl−$TaCl_4$ are from Behrens and Feber,[2] while $TaCl_5$ is from JANAF.[1]

the value adopted by Behrens and Feber.[2] We note that their alternative approach gave values that were 12−25 kcal/mol more negative. They were clearly correct to rule out the more negative values, but our results suggest that even their best estimate is too negative. Using the heats of formation for $TaCl_5$ and $TaCl_4$, they estimated values for TaCl, $TaCl_2$, and $TaCl_3$. Considering that we disagree with their value for $TaCl_4$, it is not surprising that we differ with their values for the species with less than four Cl atoms. Also included in the table are the bond energies at 298 K, BE(298). We note that our computed $TaCl_n$ bond energies follow the same general trend as the computed and experimental results for TaF_n, while the values given by Behrens and Feber do not. For example, Behrens and Feber find the first two bond energies to be larger than the remaining three, whereas the other results suggest the second bond energy is the largest followed by the third. We therefore conclude that our scaled values for $TaCl_n$ are probably the most consistent and reliable currently available.

Using our computed results, the heat capacity, entropy, and heat of formation are determined for 300−4000 K. The parameters obtained from the resulting fits can be found on the web.[32]

IV. Conclusions

The DFT atomization energies for TaF_n, $n = 1-5$, and $TaCl_5$ at both the BP86 and B3LYP levels of theory have nontrivial errors. Adding on the spin−orbit effects alone does not significantly improve the accuracy. Scaling the results using the experimental atomization energy of TaX_5 appears to significantly improve the results. CCSD(T) calibration calculations for TaF, TaCl, and $TaCl_2$ support the scaled DFT results. Using the scaled results, the computed frequencies, geometry, and spin−orbit level, the heat capacity, entropy, and heat of formation are determined for 300−4000 K. The parameters obtained from the resulting fits can be found on the Web.[32]

Acknowledgment. The author acknowledges helpful discussions with Don Hildenbrand and Ken Dyall.

References and Notes

(1) Chase, M. W., Jr.; Davies, C. A.; Downey, J. R., Jr.; Frurip, D. J.; McDonald, R. A.; Syverud, A. N. *J. Phys. Chem. Ref. Data* **1985**, *14*, Suppl. 1.

(2) Behrens, R. G.; Feber, R. C. *J. Less-Common Met.* **1980**, *75*, 281.

(3) Lau, K. H.; Hildenbrand, D. L. *J. Chem. Phys.* **1979**, *71*, 1572.

(4) Becke, A. D. *Phys. Rev. A* **1988**, *38*, 3098.

(5) Perdew, J. P. *Phys. Rev. B* **1986**, *33*, 8822 and *34*, 7406 (E).

(6) Becke, A. D. *J. Chem. Phys.* **1993**, *98*, 5648.

(7) Stephens, P. J.; Devlin, F. J.; Chabalowski, C. F.; Frisch, M. J. *J. Phys. Chem.* **1994**, *98*, 11623.

(8) Frisch, M. J.; Pople, J. A.; Binkley, J. S. *J. Chem. Phys.* **1984**, *80*, 3265 and references therein.

(9) Wadt, W. R.; Hay, P. J. *J. Chem. Phys.* **1985**, *82*, 284 and **1985**, *82*, 299.

(10) Hess, B. A. *Phys. Rev. A.* **1986**, *33*, 3742.

(11) Dunning, T. H., Jr. *J. Chem. Phys.* **1989**, *90*, 1007.

(12) Kendall, R. A.; Dunning, T. H., Jr.; Harrison, R. J. *J. Chem. Phys.* **1992**, *96*, 6796.

(13) Woon, D. E.; Dunning, T. H., Jr. *J. Chem. Phys.* **1993**, *98*, 1358.

(14) Woon, D. E.; Peterson, K. A.; Dunning, T. H., Jr., unpublished work.

(15) Dyall, K. G., personal communication.

(16) Bartlett, R. J. *Annu. Rev. Phys. Chem.* **1981**, *32*, 359.

(17) Knowles, P. J.; Hampel, C.; Werner, H.-J. *J. Chem. Phys.* **1993**, *99*, 5219.

(18) Raghavachari, K.; Trucks, G. W.; Pople, J. A.; Head-Gordon, M. *Chem. Phys. Lett.* **1989**, *157*, 479.

(19) Watts, J. D.; Gauss, J.; Bartlett, R. J. *J. Chem. Phys.* **1993**, *98*, 8718.

(20) Ross, R. B.; Powers, J. M.; Atashroo, T.; Ermler, W. C.; LaJohn, L. A.; Christiansen, P. A. *J. Chem. Phys.* **1990**, *93*, 6654.

(21) Andrae, D.; Haeussermann, U.; Dolg, M.; Stoll, H.; Preuss, H. *Theor. Chim. Acta* **1990**, *77*, 123.

(22) Martin, J. M. L. *Chem. Phys. Lett.* **1996**, *259*, 669.

(23) Helgaker, T.; Klopper, W.; Koch, H.; Noga, J. *J. Chem. Phys.* **1997**, *106*, 9639.

(24) Moore, C. E. 1949 Atomic energy levels, Natl. Bur. Stand. (US) circ. 467.

(25) Pacios, L. F.; Christiansen, P. A. *J. Chem. Phys.* **1985**, *82*, 2664.

(26) Faegri, K., personal communication.

(27) Frisch, M. J.; Trucks, G. W.; Schlegel, H. B.; Gill, P. M. W.; Johnson, B. G.; Robb, M. A.; Cheeseman, J. R.; Keith, T.; Petersson, G. A.; Montgomery, J. A.; Raghavachari, K.; Al-Laham, M. A.; Zakrzewski, V. G.; Ortiz, J. V.; Foresman, J. B.; Cioslowski, J.; Stefanov, B. B.; Nanayakkara, A.; Challacombe, M.; Peng, C. Y.; Ayala, P. Y.; Chen, W.; Wong, M. W.; Andres, J. L.; Replogle, E. S.; Gomperts, R.; Martin, R. L.; Fox, D. J.; Binkley, J. S.; Defrees, D. J.; Baker, J.; Stewart, J. P.; Head-Gordon, M.; Gonzalez, C.; Pople, J. A. *Gaussian 94*, revision D.1; Gaussian, Inc.: Pittsburgh, PA, 1995.

(28) Frisch, M. J.; Trucks, G. W.; Schlegel, H. B.; Scuseria, G. E.; Robb, M. A.; Cheeseman, J. R.; Zakrzewski, V. G.; Montgomery, J. A., Jr.; Stratmann, R. E.; Burant, J. C.; Dapprich, S.; Millam, J. M.; Daniels, A. D.; Kudin, K. N.; Strain, M. C.; Farkas, O.; Tomasi, J.; Barone, V.; Cossi, M.; Cammi, R.; Mennucci, B.; Pomelli, C.; Adamo, C.; Clifford, S.; Ochterski, J.; Petersson, G. A.; Ayala, P. Y.; Cui, Q.; Morokuma, K.; Malick, D. K.; Rabuck, A. D.; Raghavachari, K.; Foresman, J. B.; Cioslowski, J.; Ortiz, J. V.; Babal, A. G.; Stefanov, B. B.; Liu, G.; Liashenko, A.; Piskorz, P.; Komaromi, I.; Gomperts, R.; Martin, R. L.; Fox, D. J.; Keith, T.; Al-Laham, M. A.; Peng, C. Y.; Nanayakkara, A.; Gonzalez, C.; Challacombe, M.; Gill, P. M. W.; Johnson, B.; Chen, W.; Wong, M. W.; Andres, J. L.; Gonzalez, C.; Head-Gordon, M.; Replogle, E. S.; Pople, J. A. *Gaussian 98*, revision A.7; Gaussian, Inc.: Pittsburgh, PA, 1998.

(29) MOLPRO is a package of ab initio programs written by H.-J. Werner and P. J. Knowles, with contributions from J. Almlöf, R. D. Amos, M. J. O. Deegan, S. T. Elbert, C. Hampel, W. Meyer, K. Peterson, R. Pitzer, A. J. Stone, and, P. R. Taylor. The closed-shell CCSD program is described in: Hampel, C.; Peterson, K.; Werner, H.-J. *Chem. Phys. Lett.* **1992**, *190*, 1.

(30) MOLECULE-Sweden is an electronic structure program written by J. Almlöf, C. W. Bauschlicher, M. R. A. Blomberg, D. P. Chong, A. Heiberg, S. R. Langhoff, P.-Å. Malmqvist, A. P. Rendell, B. O. Roos, P. E. M. Siegbahn, and P. R. Taylor.

(31) Kee, R. J.; Rupley, F. M.; Miller, J. A. Sandia National Laboratories, SAND87-8215B 1991.

(32) The values can be found at http://www.ipt.arc.nasa.gov.